SUPPLEMENTARY DATA

Supplementary Figure 1. Stability testing of celastrol in DMSO and DMSO-PBS using ^{1}H-NMR
(a-d) ^{1}H-NMR spectra of celastrol in (a) pure DMSO-d6, (b) PBS with 50% DMSO-d6, (c) PBS with 10% DMSO-d6 and (d) PBS with 5% DMSO-d6 after 0 (blue), 7 (red) and 14 (green) days of incubation at 37°C. The spectra show superimposition of the aromatic region of celastrol over time. A decrease in the intensity of the peaks indicates that the amount of soluble celastrol has decreased over time.

(e-g) ^{1}H-NMR spectra of celastrol (aromatic region) in pure DMSO-d6 (black), PBS with 50% DMSO-d6 (red), 10% DMSO-d6 (green), 5% DMSO-d6 (blue) recorded at time 0 (e), day 7 (f) and day 14 (g). A decrease in the intensity of the peaks indicates that the amount of soluble celastrol has decreased over the time.

The decrease in peak intensity of celastrol dissolved in PBS with 50% DMSO-d6 (red) (b; red spectra in (e,f,g) points to a reaction of celastrol with degradation products of DMSO, which likely appears as new peaks for reaction products between 5 and 6 ppm.

SUPPLEMENTARY DATA

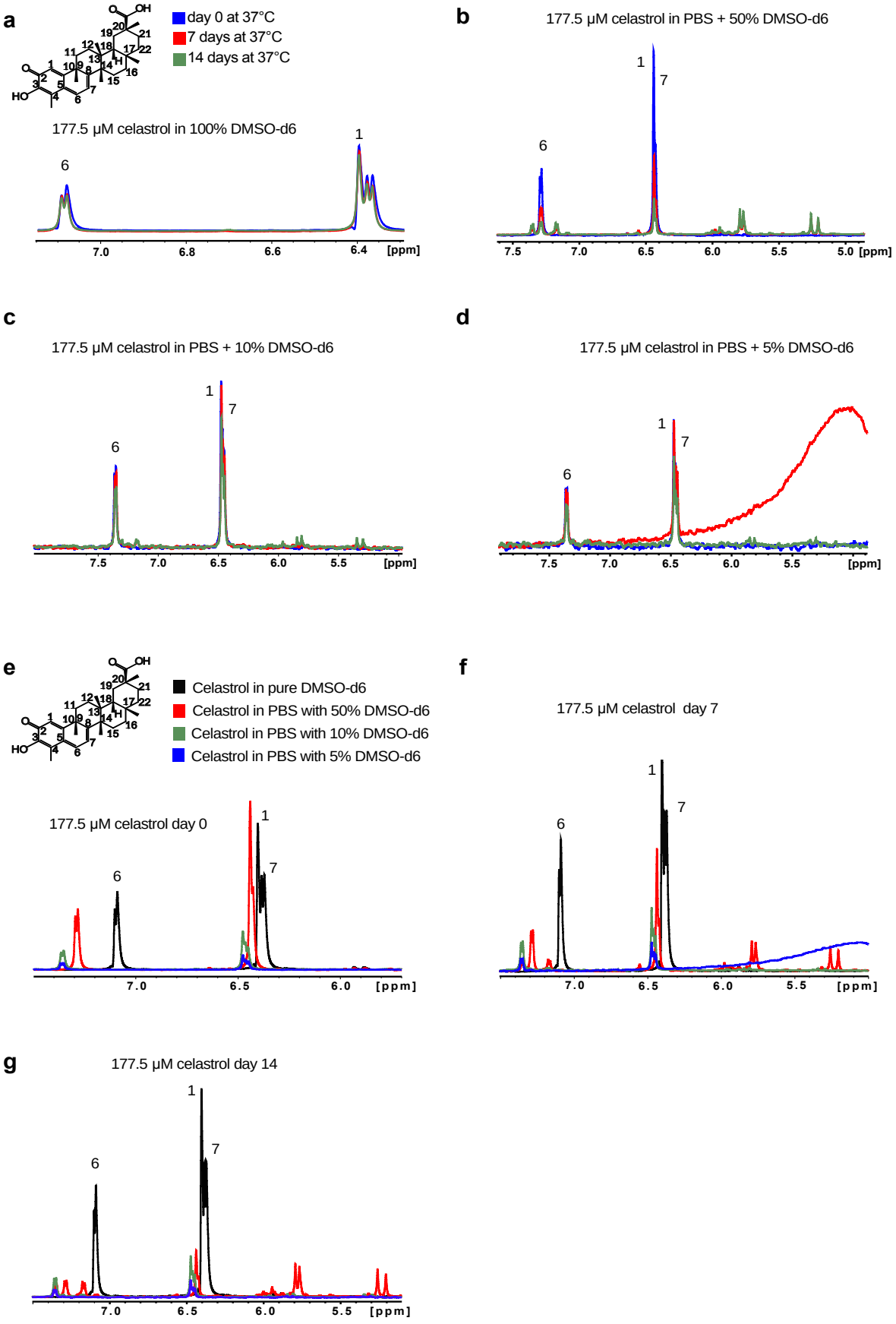

SUPPLEMENTARY DATA

Supplementary Figure 2. Celastrol reduces food intake and locomotor activity in chow- and HFD-fed mice.

(a,b) Starting body weights of male HFD-fed DIO (a; n=7) and chow-fed (b; n=8) C57Bl/6J mice injected daily with 100 µg/kg BW/d celastrol or vehicle (ip).

(c-e) Cumulative food intake (c) and average (mean per animal over 3 nights, from second to fourth night) food intake in the light (d) and dark phase (e) of male DIO mice injected daily (see arrow) with 100 µg/kg BW/d celastrol or vehicle (ip) for 4 d (n=6).

(f,g) Corresponding respiratory exchange ratios (RER), average values for the light phase and the first and second half of the dark phase (3 days and 4 nights; n=6-7) (d) and locomotor activity patterns and average values for the light phase and the first and second half of the dark phase (3 days and 4 nights; n=6-7) of vehicle or celastrol-treated mice (e).

Two-Way ANOVA with Bonferroni post-hoc tests were applied on c and g (left panel). Unpaired students t-tests were applied on a, b, d, e, f and h. Means ± SEM; *P<0.05; **P<0.01; ***P<0.001.

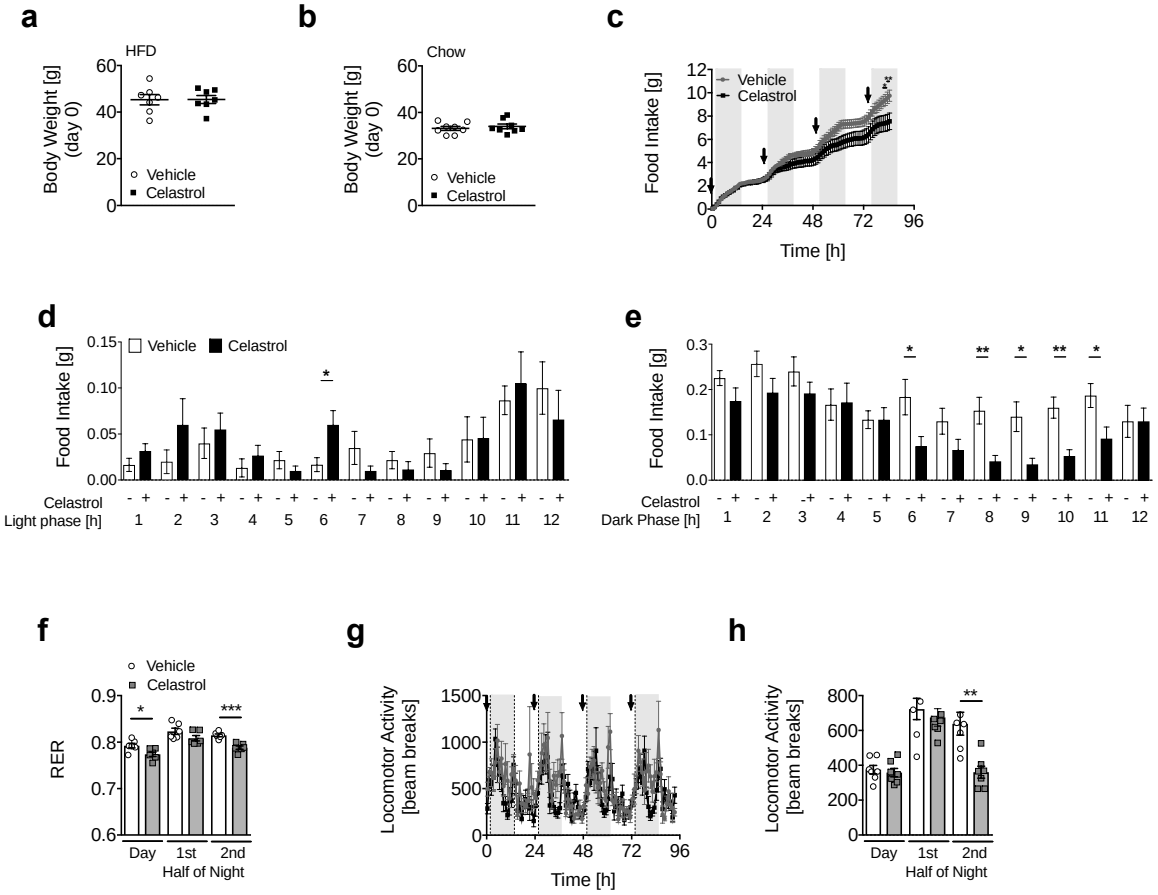

SUPPLEMENTARY DATA

Supplementary Figure 3. Celastrol actions in leptin (receptor) deficient mice

(a,b) Starting body weights of male chow-fed WT or Lep^{db}mice (a; n=4; age 8 weeks) and WT or Lep^{ob}mice (b; WT: vehicle n=8, celastrol n=8; Lepob: vehicle n=5, celastrol n=6; age: 14 ± 2 wk) at day 0 of daily vehicle or celastrol (100 µg/kg BW/d, ip) injections.

(c-f) Young male, chow-fed Lep^{ob} mice (n=8) with an age of 6 wk and with similar starting body weights (c; BW day 0) were treated with vehicle or celastrol (100 µg/kg BW/d, ip) for 7 days to monitor celastrol-induced reductions in body weight (d), fat and lean mass (e) and food intake (f; n=4 cages).

Unpaired students t-tests were applied on a, b, c and e. Two-Way ANOVA with Bonferroni post-hoc tests were applied on d and f. Means ± SEM; *P<0.05; **P<0.01; ***P<0.001.

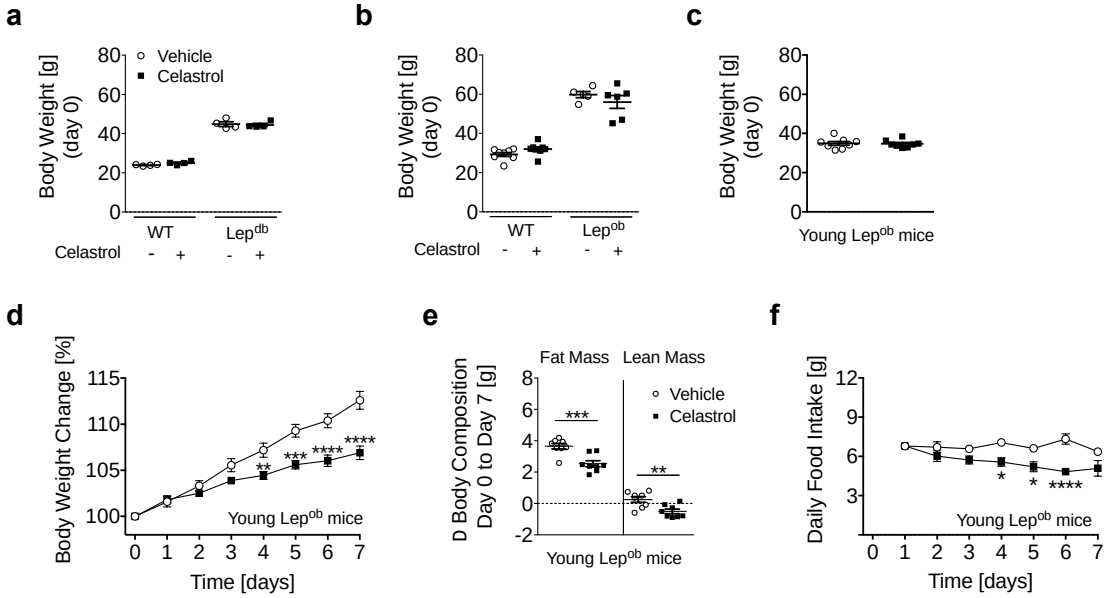

SUPPLEMENTARY DATA

Supplementary Figure 4. Effect of celastrol treatment on hypothalamic inflammatory networks, leptin signaling components and genes involved in ER stress.

(a-c) Impact of celastrol (100 µg/kg BW/d for 6 d, ip, DIO mice, n=7-8) on hypothalamic mRNA levels of (a) pro-opiomelanocortin (Pomc), cocaine- and amphetamine-regulated transcript (Cart), agouti-related protein (Agrp) and neuropeptide Y (Npy); (b) genes involved in anorexigenic-, orexigenic- and leptin signaling, i.e. melanocortin-3-receptor (Mc3r), melanocortin-4-receptor (Mc4r), leptin receptor (LepR), signal-transducer-and-activator of transcription-3 (Stat3), forkhead box O1 (Foxo1), suppressor-of-cytokine signaling-3 (Socs3), protein tyrosine phosphatase 1B (Ptp1b), t-cell protein tyrosine phosphatase (Tcptp) and Src-homology 2 domain-containing phosphatase 2 (Shp2); (c) genes involved in endoplasmatic reticulum (ER) stress (spliced form of X-box binding protein 1 (sXbp1), Xbp1, activating transcription factor 4 (Atf4), binding immunoglobulin protein (Bip), CCAAT-enhancer-binding protein homologous protein (Chop), endoplasmic reticulum-localized DnaJ4 (Erdj4)) and inflammation (interleukin-1 beta (Il1β), interleukin-6 (Il6) and tumor necrosis factor (Tnf)) (n=7-8).

(d,e) Day 0 body weights at the start of seven daily vehicle or celastrol (100 µg/kg BW/d, ip) injections in male WT (vehicle &celastrol: n=7) and PTP1B KO mice (vehicle &celastrol: n=5) that were initialy fed chow diet (d; age: 22 ± 7 wk) and subsequently subjected to 8 wk of HFD feeding (e).

Unpaired students t-tests were applied on a, b, c, d, e. Means ± SEM; *P<0.05; **P<0.01; ***P<0.01; **P<0.01.

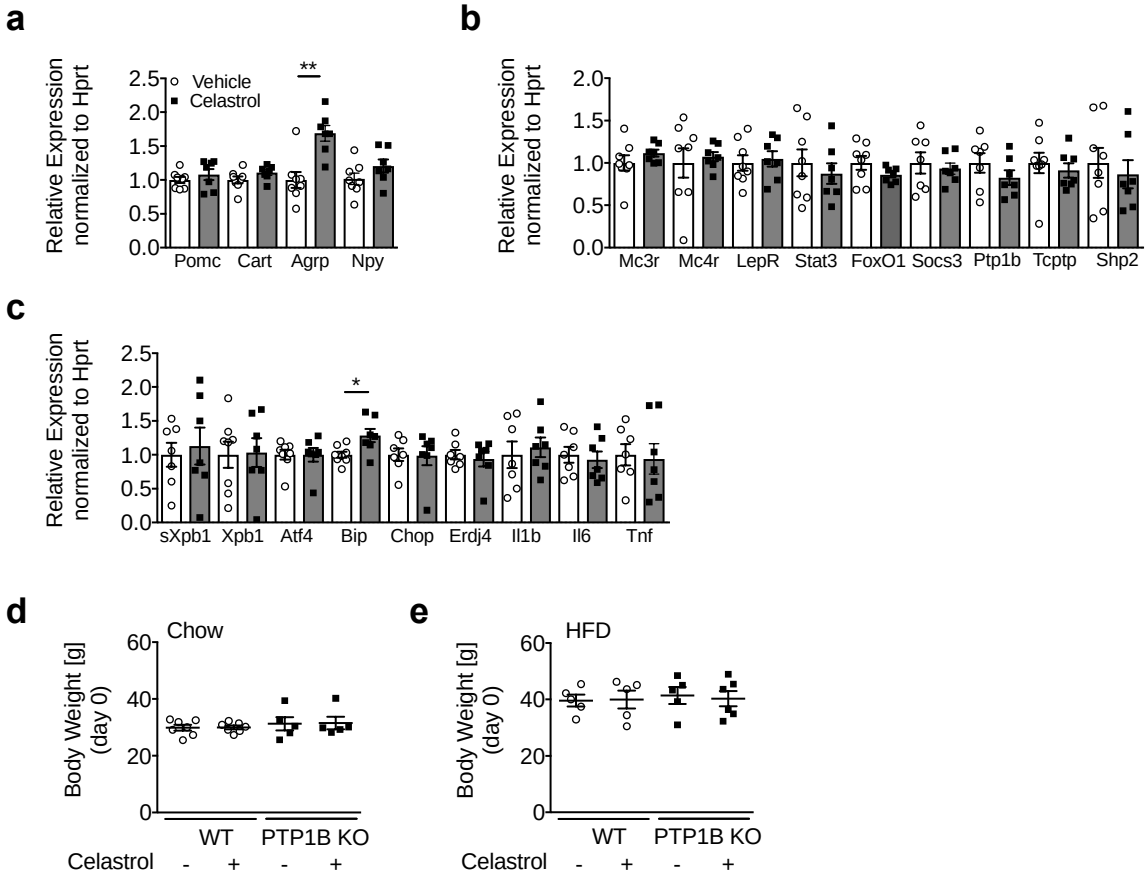

SUPPLEMENTARY DATA

Supplementary Figure 5. Effect of celastrol on key regulators of adipose tissue and skeletal muscle metabolism.

(a,b) mRNA levels of genes involved in browning, mitochondrial function, β-oxidation and heat shock response in (a) inguinal white adipose tissue (iWAT) and (b) brown adipose tissue (BAT) of celastrol vs. vehicle-treated (ip) DIO mice. PR domain containing 16 (Prdm16), cell death-inducing DFFA-Like Effector A (Cidea), peroxisome proliferator-activated receptor gamma coactivator 1-alpha (Pgc-1α), cytochrome c (Cyt c), cytochrome oxidase 4 β (Cox4), medium-chain-acyl-CoA-dehydrogenase (Mcad) and heat shock factor 1 (Hsf 1) (n=6-8).

(c,d) Oxygen consumption rates (OCRs) in C2C12 cells treated with increasing amounts of celastrol. (c) Oligomycin, Carbonyl cyanide-4-(trifluoromethoxy)phenylhydrazone (FCCP) and Antimycin A (AA), Rotenone (Rtn) and 2-deoxy glucose (2Deoxy) were added to delineate the impact of celastrol on ATP synthase activity, maximum respiration and non-mitochondrial respiration, respectively. Initial differences in basal respiration result from using wells at the border vs. the inside of the plates. OCRs were (d) normalized to the value measured at the time when celastrol was added.

(e) Expression levels of genes involved in mitochondrial function; i.e. Pgc-1α, Cyt c, Cox4β, mitofusin-1 (Mfn1) and mitofusin-2 (Mfn2), in gastrocnemii of DIO mice treated with celastrol or vehicle (ip) for 6 d (n=7-8).

(f) Expression levels of sarcoplasmic reticulum genes Ca2+ ATPase transporting cardiac muscle fast twitch 1 (Atp2a1), Ca2+ ATPase transporting cardiac muscle slow twitch 2 (Atp2a2), Ca2+ ATPase transporting ubiquitous (Atp2a3), inositol 1,4,5-triphosphate receptor 1 (Itpr1), inositol 1,4,5-trisphosphate receptor 3 (Itpr3), sarcolipin (Sln), solute carrier family 8 (sodium/lithium/calcium exchanger) member B1 (Slc8b1) and phospholamban (Plb) in gastrocnemii of DIO mice treated with celastrol or vehicle (ip) for 6 d (n=8).

(g) Starting body weights of male HFD-fed DIO mice (age: 16 wk) that were subjected to daily vehicle (n=8) or celastrol (n=9; 100 µg/kg BW/d; ip) injections or to daily vehicle injections plus pair-feeding to the reduced average calorie-intake of the celastrol-treated mice (vehicle pair-fed; n=8).

(h) Starting body weights of male HFD-fed DIO WT and UCP1 KO mice (n=7; age 44 ± 4 wk) that were subjected to daily injections of vehicle or celastrol (100 µg/kg BW/d; ip).
Students t-tests were applied on a, b, e, f, g and h. Means ± SEM; *P<0.05.

SUPPLEMENTARY DATA

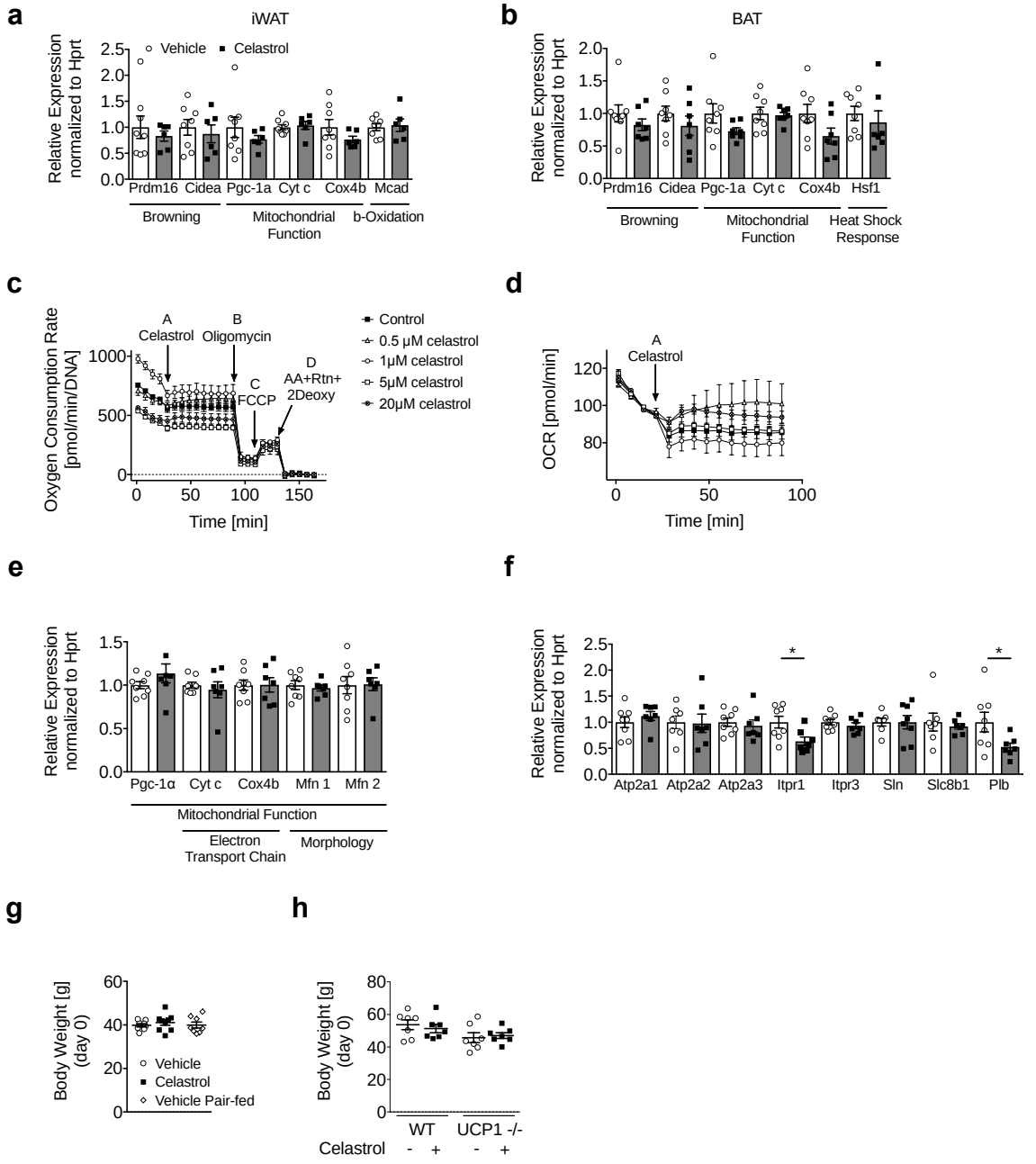

SUPPLEMENTARY DATA

Supplementary Table 1. Stability test for a 177.5 µM solution of celastrol in different solvents at day 0, 7 and 14 by NMR. The stability is calculated based on the ratio between peak intensity of the aromatic proton 6 of celastrol in PBS solution divided by the peak intensity of the same celastrol proton in pure DMSO-d6 at time 0.

	Day0	**Day7**	**Day14**
PBS + solvent	H6 Peak Intensity celastrol in pure DMSO Day 0 / H6 Peak Intensity celastrol Day0	H6 Peak Intensity celastrol in pure DMSO Day 0 / H6 Peak Intensity celastrol Day0	H6 Peak Intensity celastrol in pure DMSO Day 0 / H6 Peak Intensity celastrol Day0
100% DMSO-d6	1.00	1.08	1.09
50% DMSO-d6	1.33	2.70	5.00
10% DMSO-d6	4.76	3.84	4.76
5% DMSO-d6	11.10	10.00	12.50

SUPPLEMENTARY DATA

Supplementary Table 2. Stability test for celastrol in different solvents at day 0, day 7 and day 14 by LC-Q-TOF-MS. The stability is calculated based on the ratio between Peak Area internal standard (IS) divided by Peak Area celastrol[a]. Every experiment was repeated in duplicate.

	Day0		**Day7**		**Day14**	
Solvent	Area IS/Area Celastrol Dilution (1:400)[b]	Area IS/Area Celastrol Dilution (1:800)[b]	Area IS/Area Celastrol Dilution (1:400)[b]	Area IS/Area Celastrol Dilution (1:800)[b]	Area IS/Area Celastrol Dilution (1:400)[b]	Area IS/Area Celastrol Dilution (1:800)[b]
Pure DMSO	1.70±0.04	1.77±0.02	2.11±0.16	2.48±0.18	2.53±0.02	2.61±0.05
50% DMSO	1.77±0.04	1.87±0.02	6.18±0.84	7.39±0.08	16.12±1.03	16.18±3.94
10% DMSO	2.75±0.2	2.96±0.08	6.16±0.88	6.41±1.53	12.69±1.1	14.03±3.11
5% DMSO	2.90±0.12	2.98±0.04	6.53±0.67	7.05±0.57	26.93±5.86	31.51±6.81
Cyclodextrin+DMSO[c]	3.47±0.15	3.91±0.62	2.40±0.19	2.39±0.3	3.61±0.43	3.86±0.47
Pure cyclodextrin[d]	8.25±0.28	8.90±0.71	3.53±0.28	5.06±1.90	5.44±0.21	6.39±1.75

[a] Initial concentration of celastrol 0.08 mg/mL
[b] The initial solution was diluted in H_2O:CH_3CN (1:1)
[c] 0.8 µL/mL DMSO + 45% PBS
[d] Cyclodextrin in 45% PBS